

6-November-2020

David Albright
Manager, Groundwater Protection Section
U.S. Environmental Protection Agency, Region IX
75 Hawthorne Street
San Francisco, California 94105

RE: Response to Technical Evaluation Comments and Information Request
#3 for Underground Injection Control (UIC) Permit Application Class VI
Pre-Construction Permit Application No. R9UIC-CA6-FY20-1

Dear Mr. Albright,

Clean Energy Systems, Inc. (CES) thanks you and the staff at the United States Environmental Protection Agency (EPA) for your consideration and review of our Class VI Pre-Construction Underground Injection Control (UIC) Permit Application for the Mendota site. Please find the attached enclosures in response to your recent Technical Evaluation Comments and Information Request #3, dated 7-October-2020, covering the proposed Operating and Reporting Conditions and the Area of Review (AoR) and Corrective Action Plan - including Computational Modeling Approach – provided in the subject permit application as Attachments A and B, respectively. CES worked with technical experts at Schlumberger to develop the responses. For completeness, we directly responded EPA's Questions/ Requests within each Enclosure, in *green font*.

The enclosures are organized into two sections. The first Enclosure addresses the EPA's Evaluation of Operating Procedures. The second Enclosure addresses the EPA's Evaluation of the AoR Delineation Modeling Approach. This enclosure begins with additional information to clarify some inconsistencies identified in the documentation. Updated tables and figures are provided in the Appendix.

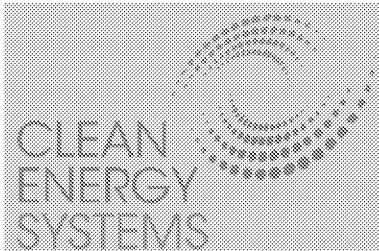
If you have any questions related to the content of this response or wish to discuss these matters further, I can be reached via email at rhollis@cleanenergysystems.com.

Sincerely,



Rebecca M. Hollis
CES Director of Business Development – CNE

www.cleanenergysystems.com
3035 Prospect Park Drive, Suite 120, Rancho Cordova, California 95670



The Power to
Reverse Climate
Change

Enclosures

CC (via email): Keith Pronske, CES President & CEO
Natalie Nowiski, Schlumberger NE CCS BD and Legal Counsel
Vivian Rohrback, Schlumberger SIS Project Manager

Table of Contents

1	ENCLOSURE 1	2
1.1	Injection Pressure	3
1.2	Annulus Pressure and Annulus/Tubing Pressure Differential.....	4
1.3	Maximum CO2 Injection Rate	6
1.4	Automated Shutdown System	6
2	ENCLOSURE 2	7
2.1	Additional Information.....	7
2.2	Evaluation of CES's Modeling	8
2.3	Evaluation of the Geomodel.....	8
2.3.1	Representation of Site Geologic Features	9
2.3.2	Representation of Hydrogeologic Properties and Lithology	9
2.4	Evaluation of the Computational Model Design.....	15
2.4.1	Spatial extent and discretization	16
2.4.2	Boundary conditions	16
2.4.3	Time steps	16
2.4.4	Model Timeframe	17
2.4.5	Initial Conditions and Operational Information.....	17
2.4.6	Relative permeability and capillary pressure curves	18
2.4.7	Potential Pathways for Fluid Movement.....	20
2.4.8	Calculation of critical pressure	20
2.4.9	Representation of Fluid Properties.....	21
2.5	Model Calibration and Sensitivity Analyses.....	22
2.6	Injection Zone Storage Capacity	23
2.7	Presentation of Model Results.....	24
2.8	AoR Reevaluation Schedule.....	24
2.9	Post-Injection Site Care Plan.....	25
2.9.1	Post-Injection Site Care Time Frame.....	25
2.9.2	Non-Endangerment Demonstration Criteria	26
3	Appendix A: Updated Tables and Figures.....	28

1 ENCLOSURE 1

Evaluation of Operating Procedures of the CES-Mendota Permit Application

This evaluation for the proposed Clean Energy Systems (CES)-Mendota Class VI geologic sequestration project summarizes the evaluation of proposed operating procedures and data submitted by CES in Attachment A to their Class VI permit application, per 146.82(a)(7),(9),(10) and 146.88. Note that this evaluation of the proposed operating conditions, particularly injection rates and pressures, was performed in conjunction with EPA's evaluation of CES's AoR delineation modeling (see Enclosure 2).

The proposed injection well operating conditions are summarized in Attachment A (the Table), as excerpted below.

PARAMETER/ CONDITION	LIMITATION or PERMITTED VALUE
Maximum Injection Pressure - Surface	2026 psig
Maximum Injection Pressure - Bottomhole	5677 psig
Annulus Pressure	2126 psig
Annulus Pressure/Tubing Differential	100 psig
Maximum CO ₂ Injection Rate	958.9 tons/day

The proposed operational procedures are also summarized in Table 20 of the Narrative, which is replicated below:

Parameters/Conditions	Limit or Permitted Value	Unit
Maximum Injection Pressure		
Surface	2026	Psi
Downhole	5677	Psi
Average Injection Pressure		
Surface	1042	Psi
Downhole	4212	Psi
Maximum Injection Rate	958.9	tons/day
Average Injection Rate	958.9	tons/day
Maximum Injection Volume and/or Mass	350000	tons/year
Average Injection Volume and/or Mass	350000	tons/year
Annulus Pressure	1142	Psi
Annulus Pressure/Tubing Differential	100	Psi

1.1 Injection Pressure

The basis for the proposed maximum injection pressure is described in Attachment A and excerpted below.

“The maximum injection pressure predicted at this pre-construction phase, which serves to prevent confining-formation fracturing, was determined: using the fracture gradient obtained from initial reservoir and geomechanical models multiplied by 0.9, per 40 CFR 146.88(a). An update to maximum injection pressure and rate will be provided once a characterization well is drilled and reservoir and geomechanical models are updated with site specific properties.”

In the Narrative, Section 7.0, second paragraph, page 85, CES notes that:

*“For the pre-construction phase the fracture pressure at the center of perforations is estimated to be **6,308 psi** at 9,705ft bgs using a gradient of **0.65 psi/ft**. A safe formation injection pressure of 90% of the fracture gradient would be **5,677 psi**. The surface injection pressure equivalent for the safe formation injection pressure assuming a **0.376 psi/ft gas** gradient (more accurate information will be gained during operation with comparison of downhole and surface sensors) would be **2,026 psi**. injection pressure to reach the 90% fracture gradient of **5,677psi** at the perforations downhole. This may change as more information is gained during the evaluation phase of the well’s geophysical properties during the drilling of the characterization well.”*

Furthermore, in the Narrative, Section 7.1, first paragraph, page 86, CES notes that:

“The maximum safe bottom-hole pressure was specified as 90 percent of the rock’s fracture pressure ($0.9 \times 0.65\text{psi/ft} = 0.585\text{psi/ft}$) at the depth where the CO₂ is injected. For conservatism, the required injection pressure was calculated based on the assumption that the required bottom-hole pressure is equal to the maximum safe bottom-hole pressure. Maximum bottom-hole injection pressure (injection depth \times 0.585 psi/ft).”

In Section 7 of the Narrative, it is not clear how CES derived or referenced the gas gradient of 0.376 psi/ft (on page 85), nor how CES has calculated the equivalent surface pressure of the maximum injection pressure of 2,026 psi.

The gradient of 0.65 psi/ft is referenced from various research papers (as noted in Attachment B, on page 17). See the AoR modeling evaluation for a discussion. The 90 percent safety factor used in Section 7 of the Narrative is consistent with the Class VI Rule at 40 CFR 146.88(a).

Questions/Requests for CES:

- Please reference the source of the gas gradient of 0.376psi/ft and/or explain its derivation.
 - *A gas gradient of 0.376 psi/ft was calculated using a steady state multiphase simulation software by using a flow of 958.9 tons per day in a 3-1/2 inch tubing with a 2.992 in internal diameter.*
- Please explain the basis for the calculation of the equivalent surface pressure of the maximum injection pressure at 2,026psi.
 - *The calculation was made using a steady state multiphase simulation software, to obtain the gas gradient for flowing CO₂ in 3.5-in. tubing to the mid-perforation depth of 9,705 ft with a maximum*

pressure of 5,677 psi. A gas gradient of 0.376 psi/ft was established by the steady state multiphase simulation software. From this, the wellhead pressure of 2,026 psi was derived.

The calculation used to obtain the surface pressure is:

Maximum surface pressure flowing = Safe bottomhole pressure flowing — (Gas Gradient * Mid-perforation depth)

Maximum surface pressure flowing = 5,677 psi — (0.376 psi/ft * 9,705 ft)

- Please describe standard operating procedures to ensure the maximum injection pressure will not be exceeded.
 - *Downhole temperature and pressure along with surface flow or mass movement, will be monitored frequently in real time at regular intervals (e.g., 1 sample/10 second rate) which will be established closer to the completion of the well. Data will be collected in an automated control system and monitored by control software that will have established thresholds for maximum injection pressure. If a threshold is exceeded, the software will issue visual, audio and digital alerts. If required, based on alert, an automatic shutdown process for the appropriate equipment will commence until the cause for any exceeded threshold is ascertained and the required corrective measures are implemented. Depending on the required time response to correct the situation the CO2 flow rate may be reduced, or CO2 equipment can be shutdown. System and software for monitoring will be established upon completion of the well.*

1.2 Annulus Pressure and Annulus/Tubing Pressure Differential

As indicated in the Table in Attachment A, the annulus pressure has been calculated as the required **100 psig** differential between the tubing and the annulus, plus the max injection pressure of 2026 psig resulting in a pressure of **2126 psig**. In contrast, in Table 20 on page 88, of the Narrative, the annulus pressure is listed as **1142 psi**.

As noted in the evaluation of the testing and monitoring plan, it appears that the annulus pressure of **2126 psig** is **higher than** the range of pressures, of **1100 psi to 1200 psi**, to be maintained in the annulus pressure monitoring system described at the bottom of page 14 of Attachment C. However, the annulus pressure of **1142 psi** listed in Table 20 of the Narrative **does** fall within the range of pressures maintained in the proposed monitoring system.

Based on a review of the collapse pressure of the injection tubing (at 10,540 psi from Table 3 of Attachment G), and the burst strength of the casing (within the range of 2440 and 12830 psi from Table 2 of Attachment G), the annulus pressure of 2026 psi is consistent with the Class VI requirements. Please see Tables 2 and 3 below.

Tubing specifications (Table 3 of Attachment G)

Name	Depth Interval (feet)	Outside Diameter (inches)	Inside Diameter (inches)	Weight (lb/ft)	Grade (API)	Design Coupling (Short or Long Thread)	Burst Strength (psi)	Collapse Strength (psi)
Injection tubing	9430	3.5	2.992	9.2	L80Cr13	Long	10160	10540

Casing specifications (Table 2 of Attachment G)

Name	Depth Interval (feet)	Outside Diameter (inches)	Inside Diameter (inches)	Weight (lb/ft)	Grade (API)	Design Coupling (Short or Long Threaded)	Thermal Conductivity @ 77°F (BTU/ft hr, °F)	Burst Strength (psi)	Collapse Strength (psi)
Conductor	86	22	21	19741	B	Welded	26.13	2440	1950
Surface	1800	16	15.01	84	N80	Long	26.13	4330	1480
Intermediate	7432	10.75	9.760	55.5	N80	Long	26.13	6450	4020
Long-stnng	7332	7	5.920	38	T-95 Type 1	Long	26.13	12830	13430
Long-stnng	10412	7	5.920	38	TN 95Cr13	Long	14.92	12830	13430

Questions/Requests for CES:

- Please explain the differences in the annulus pressures listed in the Table in Attachment A and in Table 20 from the Narrative. Please explain how each value was determined.
 - *Data for the annulus pressure in both tables are incorrect. The annulus pressure should be generated by a CO₂-inhibited fluid of a density of approximately 11.45 ppg to 9,702 ft to a pressure above the packer of 5,777 psi. This will deliver a positive pressure of 100 psi above the packer with a 5,677-psi injection pressure. Attachment A: Summary of Requirements Class VI Operating and Reporting Conditions table and Table 20 in the Class VI Permit Application Narrative 40 CFR 146.82(a) will be updated accordingly. Please refer to Appendix A for updated tables.*
- Please describe standard operating procedures to ensure the maximum annulus pressure will not be exceeded.
 - *Surface wellhead and downhole conditions will be monitored continuously for pressure. Thresholds will be established based on limitations of well equipment and geological concerns downhole with respect to the maximum allowable pressures. These thresholds cannot be established until the well is drilled and analysis of the formation is performed and understood. After a threshold is achieved or exceeded, the system will deliver alarms to indicate there is an issue. Resolution will depend on the type of alarm and systems installed to regulate pressures. Typically, a list of options will be provided to the operator as to what could cause a high-pressure event. Shutdown will need to be gradual so that monitoring of the pressures and changes can be evaluated to determine if there is impact to the well or formation. Depending on the scenario, it*

may be necessary to vent well fluids to a predetermined safety location. This option would be considered as a process of last resort in maintaining pressures inside the wellbore's specifications.

1.3 Maximum CO2 Injection Rate

CES proposes a maximum daily CO2 injection rate of 958.9 tons per day, which equates to 350,000 tons/year (or 4.2 million tons over 12 years or 7 million over 20 years). See the modeling evaluation report (Enclosure 2) for additional discussion.

Questions/Requests for CES:

- Please describe standard operating procedures to ensure the maximum daily injection rate will not be exceeded.
 - *Surface wellhead and downhole conditions will be monitored continuously. Injection rate or mass flow is one of the parameters to be monitored at surface. Thresholds will be established based on limitations of well equipment and geological concerns downhole with respect to the maximum injection rate. These thresholds cannot be established until the well is drilled and analysis of the formation performed and understood. After a threshold is achieved or exceeded, the system will deliver alarms to indicate there is an issue. Resolution will depend on the type of alarm and systems installed to regulate the injection rate. Typically, this will require a reduction in the injection rate without the need for a shutdown. But the situation must be reviewed to understand what systems failed or did not perform properly and thus created an excessive injection rate.*

1.4 Automated Shutdown System

According to Section 7, page 85, of the Narrative, CES plans to connect the information system collecting data from the pressure, temperature and mass flow gauges/sensors with automatic controls “to assist with shut down or flow controls if certain critical parameters are reached such as Maximum Flow Rate, or Pressures and Temperatures at surface and downhole...” CES notes the automatic control system is not yet defined, as more details are needed to properly implement.” This system will be evaluated when CES provides additional information.

Questions/Requests for CES:

- Please include standard operating procedures supporting the automated shutdown system when details about the system are provided.
 - *Downhole temperature and pressure along with surface flow or mass movement, surface pressure, and temperatures will be monitored in real time at frequent rates (i.e., typically 1 recording 10 /seconds, rate not established yet). Data will be collected in an automated system and monitored by control software that will have thresholds established in it. After a threshold is seen or exceeded, the software will issue visual, audible, and digital alerts and/or begin with an unload procedure and transition into the shutdown process for appropriate equipment until it is understood why the thresholds were achieved and what corrective measures must be implemented. System and software for monitoring has not been established yet. Currently, data acquisition and monitoring systems are not adequately defined as to what specific procedures are followed to initiate an automatic shutdown.*

2 ENCLOSURE 2

Evaluation of the AoR Delineation Modeling Approach for CES-Mendota Class VI Permit Application

This area of review (AoR) delineation modeling evaluation report for the proposed Clean Energy Systems (CES)-Mendota Class VI geologic sequestration project summarizes EPA's evaluation of the modeling performed by CES as described in the Area of Review and Corrective Action Plan (Attachment B of the permit application). This review also addresses modeling-relevant site characterization information in the permit application narrative and associated files submitted to the GSDT per 40 CFR 146.84. Because they are related, this report also addresses certain elements of the proposed Post-Injection Site Care Plan (Attachment E of the permit application) that are based on the AoR modeling results. Clarifying questions for CES are provided in blue within the text below.

This report describes and evaluates how site-specific data (e.g., geologic data and planned operational conditions) described in the UIC permit application are incorporated into CES's geomodel and their computational modeling approach. Note that EPA did not perform independent, duplicative modeling of CES's AoR. Based on the breadth of currently available site-specific data and the description of the modeling effort as provided in the permit application materials, this is not warranted at this time. It is assumed that planned pre-operational testing will confirm the site characterization.

2.1 Additional Information

The EPA identified inconsistencies within Enclosure 2, which Clean Energy Systems would like to clarify below in Table 1.

Table 1: Summary of Inconsistencies Addressed

Section	EPA Inconsistency (in Black Text)	CES Clarification
2.3	"and data for well tops obtained from California Geologic Energy Management Division (CalGEM, previously known as DOGGR), Seismic Exchange, Inc (SEI), or Information Handling Services (IHS)"	<i>Well tops were obtained from CalGEM and IHS.</i>
2.3.1	"These include the roughly 1,000 ft. thick Moreno Shale (the primary confining zone), the First Panoche Sand, the ~100 ft. thick first Panoche Shale (initial confining zone), the >1,000 ft. thick Second Panoche Sand (primary injection zone), and the underlying formations, including the 1,400-2,500 ft. thick Fourth Panoche Sand (the secondary injection zone)."	<i>The Moreno Shale is the secondary confining zone, and the First Panoche Sand is the secondary injection interval (dissipation zone). The primary seal is the First Panoche Shale. The Fourth Panoche Sand is a potential alternative injection target, if it is present at the injection site.</i>
2.3.1	"The upscaled porosity and permeability graphics in Attachment B (Figures 3 and 4) would benefit from labeling for formation tops."	<i>The figures were updated with formation tops in Figure 7 and Figure 8 (refer to Appendix A).</i>

Section	EPA Inconsistency (in Black Text)	CES Clarification
2.3.2.2	“based on well logs from the NAPA AVE A 1 well, about 3 mi to the east of the injection well (narrative page 51)”	<i>The NAPA AVE A/1 is located approximately 8.3 miles to the east.</i>
2.4.7.2	“Within a 2.5-mile radius”...	<i>A 5-mile radius was used to calculate pore volume.</i>
2.9.1	“CES proposed a 10-year alternative post injection site care time frame but did not provide a justification for the appropriateness of the 10-year time frame that addresses the criteria at 40 CFR 146.93(c).”	<i>For the pre-construction application, a 10-year post-injection was proposed based on the stabilization of simulated plume and pressure AoR within the 10-year post-injection time frame. See Figures 2 thru 7 in Attachment C: Testing and Monitoring plan for the temporal evolution of AoRs. As stated in the application, this post injection site care (PISC) time frame will be re-evaluated and updated accordingly after site-specific data are collected.</i>

2.2 Evaluation of CES’s Modeling

CES used Petrel for developing the geomodel and the ECLIPSE reservoir simulator for numerical simulations of plume and pressure front development. Petrel is a software platform that supports development of a site geomodel, allowing synthesis and 3-D visualization of data on reservoir characteristics (e.g., seismic data, structural features, well data, upscaled well properties). Use of ECLIPSE for numerical simulations is consistent with the requirements of the Class VI Rule at 40 CFR 146.84. It accounts for the multi-phase nature of the injection activity and for the physical and chemical properties of all phases of the injected carbon dioxide (CO₂) stream and displaced fluids. It allows for modeling of geochemical reactions associated with geologic sequestration of CO₂. Use of these modeling programs is appropriate for simulations of plume and pressure front at a GS site.

2.3 Evaluation of the Geomodel

CES developed a geocellular model (geomodel) to support the numerical modeling using Petrel. The geomodel incorporates available data sources, including well logs from ten existing wells within several miles of the proposed injection well, 2D seismic data, and data for well tops obtained from California Geologic Energy Management Division (CalGEM, previously known as DOGGR), Seismic Exchange, Inc (SEI), or Information Handling Services (IHS). These data are synthesized to represent the subsurface system and initial conditions in a 3D grid. The geomodel for the Mendota site was used to represent the extent and thickness of the injection and confining zones with upscaled log data for petrophysical properties. Section 2.4.3 (page 39 of the narrative) states that the lateral grid resolution (cell size) for the geomodel is 400 ft. by 400 ft. CES intends to use a finer resolution for the grid when 3D seismic data (to be acquired later in the project) can be incorporated into the geomodel. Layer increments are 4 ft.

The discussion below of the site-specific parameters that CES used to build the geomodel expand on the geologic site characterization presented in the permit application narrative.

2.3.1 Representation of Site Geologic Features

The geological layering, formation thicknesses, and petrophysical properties of the project site (as described in the permit application narrative and evaluated in the geologic site characterization report) need to be integrated into a geomodel and then a numerical model domain that is consistent with available information to generate predictions of plume and pressure front movement.

The geomodel model is used to represent the depth, areal extent, and thicknesses of the injection and confining zones at the CES-Mendota site based on the site-specific data described above. These include the roughly 1,000 ft. thick Moreno Shale (the primary confining zone), the First Panoche Sand, the ~100 ft. thick first Panoche Shale (initial confining zone), the >1,000 ft. thick Second Panoche Sand (primary injection zone), and the underlying formations, including the 1,400-2,500 ft. thick Fourth Panoche Sand (the secondary injection zone). The formation thicknesses and regional dip shown in the domain for the numerical model (Model-Domain file) submitted to the GSDT are derived from the geomodel and reflect the current understanding of the Mendota site.

The porosity and permeability data from the 10 wells in the surrounding area (average values summarized in Table 3 of the narrative) were used to develop the porosity and permeability distributions in the geomodel (Figures 28, 31, and 34-39 of the narrative) from the Garzas formation down through the Precambrian basement. Visual inspection shows the values in the color legend in these figures to be generally consistent with the values in Table 3.

Figures 3 and 4 of Attachment B show cross sections of upscaled porosity and permeability distributions developed for the ECLIPSE modeling. The porosity distribution agrees well visually with the geomodel and well data.

In general, the available geologic site characterization data with respect to layering, thicknesses, and depths appear to have been rendered as faithfully as possible in the geomodel and subsequently for use in the numerical modeling (as shown in the Model-Domain file). The upscaled porosity and permeability graphics in Attachment B (Figures 3 and 4) would benefit from labeling for formation tops. It is assumed that the workflow used to generate the geomodel and numerical model domain will produce as reasonable representations of the subsurface as possible as new data become available.

2.3.2 Representation of Hydrogeologic Properties and Lithology

2.3.2.1 Porosity, permeability, and rock types

Effective porosity was determined using either bulk density or compressional slowness (from acoustical logs), combined with an estimate of irreducible water (narrative Section 2.4.2.1; discussed in the review of site characterization data). Intrinsic permeability was based on the porosity and lithology (narrative Section 2.4.2.2); CESs reference Herron (1987). The petrophysical properties (effective porosity, permeability, clay volume, and pore volume) were then upscaled from log data into 4 ft. layers along the wellbore.

- Do the permeability data represent horizontal permeability?
 - *Permeability was calculated using bulk density and calibrated to core data from NAPA AVE A/I. The core data were not tested for a specific direction. For the dynamic modeling, the permeability was assumed to represent the horizontal permeability. The vertical anisotropy (k_v/k_h) was assumed to be 0.1.*
- What method was used to upscale the petrophysical properties along the wellbores of the 10 wells for which logging data were used? How was upscaling handled for the different formations? How was the success of this method evaluated?
 - *Effective porosity and permeability were upscaled using arithmetic averaging methods. Although the geometric mean upscaling method can be used for permeability, in this case, the arithmetic method was most representative of the well logs. Please refer to Figure 1 and Figure 2 in Appendix A. Layer thicknesses are constant per modeled zone. Upscaling results were quality checked using histograms and crossplots comparing the raw and upscaled data. Histograms and crossplots show a reasonable match throughout the modeled zones.*

Once upscaled, the petrophysical properties were distributed into the geomodel through Gaussian Random Function Simulation, a kriging-based algorithm (narrative Section 2.4.3). CES notes that facies logs were not used as bias in the current porosity or permeability models, but that facies biasing and Kriging to 3D seismic data will be considered in future model iterations. Figure 28 in the narrative (page 42) shows the modeled average porosity maps for each formation.

- Figure 26 in the narrative shows the net thickness maps of the Moreno Shale and First and Second Panoche Sands. The proposed injector is close to the western edge of the maps. Will the formation thicknesses further to the west of the injector be able to be represented when the 3D seismic data have been acquired?
 - *Petrophysical well log data availability is limited to the east side of the model domain near legacy oilfields. 3D seismic interpretation will provide additional structure to characterize formation thicknesses to the west and south, where the current data are limited.*
- All but one of the wells with logs used to support development of the petrophysical property distributions in the geomodel are more than 3 miles from the injector (narrative Figures 28 and 31). While crucial site-specific data will be collected when Mendota INJ_1 and OBS_1 are drilled, they will provide only two data points. How will updates to the geomodel reflect a sufficient level of detail throughout the AoR?
 - *The 3D seismic data will assist in defining the structure throughout the AoR as well as provide insight on the continuity of injection and sealing formations. Logs collected at Mendota_INJ_1 and OBS_1 (and the other seven petrophysical wells where density is available) will be used for simultaneous seismic inversion and the generation of probably based lithology (sandstone, shale) cubes.*

The graphs in Figure 30 of the narrative compare the combination of porosity and permeability of the upscaled cells and modeled cells, porosity vs. permeability by zone/formation, and porosity vs. permeability for two lithologies (sand and shale).

- In the plot of well log-derived data points, upscaled values, and full-field simulated cells, the

upscaled values dominate. It appears that the upscaled value symbols may have been layered over the other symbols. Please revise the figure to show the distributions of all three types of data points more clearly.

• *For clarity, Figure 30 has been subdivided into three figures. Please refer to Figure 3, Figure 4, and Figure 5 in Appendix A.*

- Are there any concerns about autocorrelation since the permeability was based on porosity and lithology? If so, how was this issue addressed?
 - *Collocated cokriging permeability to porosity is a best practice in scenarios where calibration data are lacking. Core samples from Mendota_INJ_1 and Mendota_OBS_1 will provide a better understanding of permeability throughout the AoR. A refined facies model will provide additional and improved data for the permeability distributions and full field model population.*
- How many core samples from NAPA AVE A/1 were used to support calibration between the core data and well logs?
 - *A total of 45 core samples were used to calibrate the well log to core data for the NAPA AVE A/1. Core depths range from 3,452 to 9,666 ft.*
- In the core-to-log calibration, how was bias between core samples and well logging data handled given that cores may not capture the heterogeneity that well logging can capture?
 - *Well log data are calibrated to core by adjusting the petrophysical model to align core variables to the petrophysical model output variables. Heterogeneous biases are resolved during the petrophysical model building process by ensuring that all existing data such as SP, resistivity, density, neutron, gamma ray, and core coincide with each other using principle component structures. Core samples are considered point data at a given depth and are used as a calibration for log models and are not an absolute. Therefore, models are never forced to match the core but rather are adjusted to obtain the best fit possible while honoring all input and output data.*

The narrative notes on page 34 that, “As shown in Table 2, some of the wells have a limited set of well log data. The petrophysical property uncertainty around these wells was reduced by calibrating parameters and multi-well comparisons across different formations.”

- Please expand on the multi-well calibration described on page 34 of the narrative. Specifically, how were these data incorporated into the geomodel in a manner that is representative of the geologic system at the proposed site?
 - *The multiwell calibration begins with log input normalization. Variables are compared from one well to another as a whole and on a zone-to-zone basis. This allows the petrophysical model to be compared comprehensively, which makes it possible to determine whether an adjustment is required due to unacceptable variability. After all wells are processed, the output variables (volume clay, porosity, and permeability) are compared against each other following a similar process to that used with the input variables. Due to limited data, there is uncertainty around the geologic system at the proposed site. The proposed location is between deltaic shelf deposits to the east (Gill Ranch) and basal turbidite fans to the west (Cheney Ranch). To be conservative, the model was developed to represent a connected geologic system. Petrophysical well log data availability is limited to the east side of the model domain; therefore, it is difficult to characterize the proposed site's exact placement within the geological system. 3D seismic data will assist in refining the geologic system at the proposed site.*

The graph in Figure 30 of the narrative showing porosity vs. permeability by formation is labeled as Z values and the legend title is “Zones.”

- Please clarify the meaning of the zones in the legend of Figure 30. Are they equivalent to the formations, as suggested by the legend?
 - *Zones are equivalent to formations. For clarity, Figure 30 has been updated and divided into Figure 3, Figure 4, and Figure 5 in Appendix A.*
- Were the data binned into zones and then associated with the specific formations? If so, please describe the method by which this association was accomplished.
 - *The petrophysical characteristics (porosity and permeability) of each zone (formation) are different. Therefore, to keep these characteristics contained within each zone, the interwell interpolation of these properties was completed on a zone-by-zone basis in the Petrel® platform.*
- Were the graphs in Figure 30 the basis for assigning phi and k in the layering in the model domain?
 - *For clarity, Figure 30 has been updated and divided into Figure 3, Figure 4, and Figure 5 in Appendix A. The graphs show the unique porosity/permeability relationships per zone. The corresponding variables were used in the layering model.*

Figure 1 in the Rock Types file submitted to the GSDT shows rock types assigned according to porosity and log k, with the shape of data spread matching Figure 30 in the narrative. The Rock Types file indicates that data were divided into two rock types (shale and sand), and relative permeability and capillary pressure curves were assigned to the two types. The rock types were defined based on the porosity and permeability data using a neural network training method.

- Were the relative permeability and capillary pressure curves the only properties assigned based on this facies assignment and the scheme in Figure 1 of the Rock Types file?
 - *Yes, the relative permeability and capillary pressure curves were the only properties assigned based upon the facies assignment.*
- Why was the information shown in Figure 30 of the narrative not used as the basis for assigning these curves?
 - *The facies model described in Figure 30 (updated with Figure 5) was a preliminary estimate to perform fault seal analysis. This facies log was not used as part of the petrophysical model interpolation. The rock classification methodology (neural network) was used to create the hydrofacies interpretation needed for dynamic modeling. Porosity and permeability of the geocellular model were upscaled to a tartan grid used for dynamic modeling. Please refer to Figure 6 in Appendix A.*
- What is the uncertainty associated with the neural network training method?
 - *Neural networks estimate discrete patterns from provided input data. Unsupervised neural networks are used to subdivide the input data into several classes. This method looks for regularities or trends in the input data. In this case, two full field properties (log permeability and porosity) were the main input data. Additional input variables, if available, would strengthen the training of the neural network because permeability was estimated using porosity, both in petrophysical estimation and full field modeling. Future methodologies for*

rock typing/classification will include heterogeneous rock analysis (HRA), lithology cube analysis, and laboratory measurements.

Figure 2 in the Rock Types file shows rock types along an E-W cross section. The cross section has two different shades of blue in addition to purple.

- Is there a difference between the two shades of blue in Figure 2 of the Rock Types file?
 - *No, the different blue shades are due to the presence of grid lines shown on the figure. Refer to Figure 6 in Appendix A for an updated version.*
- Please label the formations in Figure 2.
 - *Refer to Figure 6 for an updated version of Figure 2 in Appendix A which includes the formation names.*

In comparing Figure 1 in the Rock Type file with Figure 30 of the narrative, the facies in Figure 30 show a broad spread rather than the sharp dividing line in Figure 1. It appears that a number of shale data points in Figure 30 were assigned to the sandstone facies by the neural network training method in Figure 1. There also appears to be a significant difference in porosity between the Fourth Panoche and the Second Panoche Sands in Figure 30.

- Are the porosity differences between the Second and Fourth Panoche Sands sufficient to possibly warrant a third rock type?
 - *The Fourth Panoche Sandstone appears more laminated in nature than the Second Panoche Sandstone, which appears blocky or channelized and which, therefore, may exhibit differences in porosity. It is possible a third, fourth, or fifth rock type will be required to characterize all zones. After additional well log data are acquired, it will then be determined how many more rock types will be defined.*
- Please discuss how these two methods of assigning facies were used to inform the geomodel and, consequently, the numerical model.
 - *The facies model described in Figure 30 (updated with Figure 5) was only constructed to characterize fault seal analysis; it was not used to inform the geomodel. The rock typing methodology with neural network was applied for the classification of hydrofacies (rock types) to assign relative permeability and capillary pressure functions in the dynamic modeling.*
- Will there be any changes to these methods in subsequent revisions to the geomodel and numerical model?
 - *Future iterations of facies modeling will rely on site-specific data such as wireline well logs and 3D seismic data. Wireline well logs such as density, neutron, and gamma ray, along with other processed variables, will be used to create an HRA discrete rock typing log. 3D seismic data and density and sonic logs will be used to create a low-frequency cube that will then inform the lithology cube analysis. This will provide a more informed understanding of the geologic system. Results of lithology cube analysis and site-specific data will determine if hydrofacies rock typing is needed for dynamic modeling.*

2.3.2.2 Geomechanical properties

At this preliminary stage, some geomechanical properties have been assumed based on well log data from nearby wells and empirical relationships. For example, density and compressional slowness in the Moreno Shale were based on well logs from the NAPA AVE A 1 well, about 3 mi to the east of the injection well (narrative page 51). Fracturing of the formation at the project site is also unknown. There are currently no laboratory core measurements for rock strength and ductility for the project site.

It is understood that the appropriate lab analyses will be performed on representative cores when the injection well and the OBS_1 deep monitoring well are drilled. It is also understood that borehole image logs will be acquired and used along with the 3D seismic imaging to develop a discrete fracture model.

2.3.2.3 Geomodel - 3D model grid resolution

The narrative notes in Section 2.4.3 that structural surfaces (i.e., formation contacts) were used to produce a basic framework for the geomodel. The lateral grid cell size was 400 ft. by 400 ft, but CES intends to use a finer grid once 3D seismic data have been acquired and incorporated.

Variogram modeling using the petrophysical logs showed “.. a NE-SW depositional trend, with a vertical resolution of roughly 20 ft. by 20 ft. is likely representative of larger depositional changes (for example from high-stand to low-stand sea level). To capture smaller changes within each depositional cycle, 4 ft layer increments were defined for each zone.”

These increments are geologically reasonable. It is understood that the geomodel will be updated and refined once new, more detailed site-specific information are available.

2.3.2.4 Fault stability

There are currently limited data to assess the stability of faults. As noted above, the application indicates that geomechanical information will be collected during the pre-operation phase via core analyses, pilot hole logs, and well tests. The narrative notes that in-situ stress can be assessed integrating the density of the rock above the depth of interest (vertical stress), and minimum and maximum horizontal stresses will be assessed via mini-frac testing and other methods. The application indicates that these new data, along with 3D seismic profiling, will allow characterization of the in-situ stress field, pore pressure, and rock strength. The geomechanical model that these data will support will be used for a more comprehensive analysis of fault stability and sealing capacity.

The application cites a study by Chiaramonte et al. (2008) describing the development and application of a geomechanical model for the Tensleep Formation to support consideration of a CO₂-GS project at Teapot Dome. Chiaramonte et al. used the geomechanical model to estimate the pore pressure that would cause fault slippage. The methods used by Chiaramonte et al. are thorough in terms of the geomechanical characterization of the site and include a probabilistic sensitivity analysis. At this point, we assume that CES intends to follow the same approach once they have the necessary data. EPA will evaluate the data, geomechanical model, and conclusions when it has been developed.

2.4 Evaluation of the Computational Model Design

As noted above and in the site characterization report, CES's modeling is based on preliminary data, which will be refined when the injection and deep observation wells are drilled and additional data (e.g., formation data and 3D seismic) are collected. Specific elements of and considerations in our review are described in the sections below.

Routines for Relevant Subsurface Processes

CES used the ECLIPSE 300 (v2018.2) reservoir simulator with the CO2STORE module to perform the AoR delineation. ECLIPSE includes routines for the relevant subsurface processes at the site, including equations of state for CO₂ and other chemical species of interest.

As Attachment B describes, "ECLIPSE 300 is a compositional finite-difference solver that is commonly used to simulate hydrocarbon production and has various other applications including carbon capture and storage modeling. The CO2STORE module accounts for the thermodynamic interactions between three phases: an H₂O-rich phase (i.e., 'liquid'), a CO₂-rich phase (i.e., 'gas'), and a solid phase, which is limited to several common salt compounds (e.g. NaCl, CaCl₂, and CaCO₃). Mutual solubilities and physical properties (e.g. density, viscosity, enthalpy, etc.) of the H₂O and CO₂ phases are calculated to match experimental results through a range of typical storage reservoir conditions, including temperature ranges between 12°C-100°C and pressures up to 60 MPa. Details of this method can be found in Spycher and Pruess (2005)."

Geochemistry was not included in the numerical modeling. The narrative does discuss the geochemical modeling that was done separately; this content was addressed in the site characterization evaluation included in EPA's technical evaluation comments and information request dated August 19, 2020. Coupled geochemistry and multiphase flow would allow exploration of potential effects of mineral dissolution and precipitation on porosity and permeability and the possible long-term effects of mineral trapping on storage capacity. We understand, however, that there can be challenges in simulating changes in petrophysical properties because of factors such as sediment texture and grain morphology.

- Will reactive transport modeling be attempted when additional data are available? If not, please explain how the lack of incorporation of geochemical reactions into the model may (or may not) limit the accuracy of the predictions of plume and pressure front migration.
 - *Geochemical batch reaction modeling based on the preliminary data indicated that there is no significant impact on the rock properties from CO₂-water-rock reactions. The formation rock is composed of a mineral assemblage commonly found in sedimentary rocks whose reaction pathways with CO₂-saturated brine are relatively well understood. After a characterization well is drilled, the site-specific data will be used with the geochemical modeling to update and evaluate the effect of geochemical reactions on petrophysical properties. Application of reactive transport modeling will be considered after the mineralogic, petrographic, and geochemical data have been reviewed and when newly found mineralogic and sedimentary characteristics could potentially lead to significant impacts.*

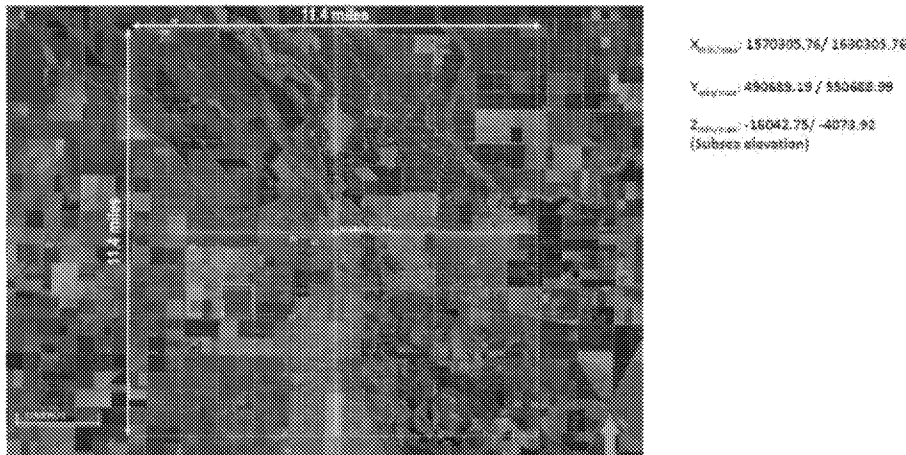
2.4.1 Spatial extent and discretization

The model domain was generated in Petrel. The static grid for the numerical model is 19 miles by 19 miles in the x and y directions. The part of the domain used for dynamic modeling is 11.4 miles by 11.4 miles in the x and y directions, with a tartan pattern of smaller cell sizes closer to the proposed injection well, as shown in Figure 1 of Attachment B, which is reproduced below.

In the Z direction, the domain includes the Garzas Formation (the first permeable sandstone above the Moreno Shale confining zone) down through the basement. The grid comprises "...53 x 53 x 446 cells (totaling 1,252,814) in the x, y, and z direction, respectively, with variable cell sizes. The smallest grid cells around the injector and observation well are 60 ft x 60 ft laterally. Vertical thickness of each cell within the model depends on the vertical proportion of each formation."

This approach to discretization appears to be generally appropriate; it is understood that the horizontal grid cell size will be reduced as appropriate based on 3D seismic data to be acquired later in the project.

Model Domain and Tartan Grid



2.4.2 Boundary conditions

Section 2.6 of Attachment B states that the upper and lower boundaries were set as no-flow boundaries assuming continuous presence of the upper and lower confining zones throughout the project area. At the horizontal boundaries, the cells were set to simulate an infinite-acting boundary by applying a pore volume multiplier of 1×10^6 for each boundary cell.

2.4.3 Time steps

Attachment B, on page 7 describes the time step selection, noting that the software optimizes the time steps to meet converge criteria. "Convergence is achieved once the model reaches the maximum tolerance where small changes of temperature and pressure calculation results occur on successive iterations. New time steps are chosen so that the predicted solution change is less than a specified target."

2.4.4 Model Timeframe

Simulations were run for 20 years of injection into the Second Panoche Sand (which is the upper end of the 12 to 20-year range described in the permit application) and out to 50 years post-injection. Map and cross-sectional views of the simulated plume and pressure front throughout this timeframe were provided in the “AoRs” file submitted in the GSDT.

2.4.5 Initial Conditions and Operational Information

The table below summarizes the initial conditions and operational information used in the computational model submitted via the GSDT. These parameters appear to be appropriate based on the baseline site characterization data and proposed operating conditions described in the permit application. A discussion of specific conditions is presented below the table.

Initial Conditions (and associated reference elevations)	Value
Reference elevation	-9505 ft MSL
Elevation of top of perforated interval	-9400 ft MSL
Composition of injectate	Pure CO ₂
Pressure gradient	0.4339 psi/ft (Attachment B, page 14)
Initial Aqueous Pressure	4,211 psi
Initial Temperature	137.5°F at -6350 ft MSL 249.7°F at -13350 ft MSL
Initial Salinity	25,000 mg/L

Operational Information	Value
Mass Rate of Injection	350,000 tons/year
Fracture Gradient	0.65 psi/ft
Maximum Injection Pressure	5677.4 psi
Elevation corresponding to pressure	-9505 ft
Composition of injectate	Pure CO ₂
Injection Schedule	Single injection Period (20 years)
Injection Start date	01/01/2021
Number of production/withdrawal wells	N/A
Pressure gradient	0.4339 psi/ft (Attachment B, page 14)

The Second Panoche Sand (the primary injection interval) is located from about 8,900-10,000 ft bgs. For most of the operational conditions in the model, a reference elevation of 9,505 ft SSTVD is used. However, it is noted that calculations based on depth (maximum injection pressure and initial aqueous pressure) use 9,705 ft KB (Attachment B, page 19). The reference elevation is located in the middle of the perforated zone which begins at 9,400 ft MSL and extends to 9,620 ft MSL (Attachment B, page 16).

Note that, if CES opts to inject into the Fourth Panoche Sand, these values would need to be revised.

The injectate as modeled is composed of pure CO₂. Table 8 of the narrative presents analysis of a

sample of the injectate, which is 96.78% CO₂ with impurities, the most notable of which is O₂ (1.15%), which is reactive with redox sensitive minerals present in the formation, and is incorporated into the geochemical model (narrative, page 64). These relatively minor impurities are not a concern for this initial round of multiphase transport modeling. If CES pursues reactive transport modeling in the future, the full composition of the injectate will need to be accurately represented.

Initial aqueous pressure and initial temperature were extrapolated using the reference elevation and DOGGR/CalGEM data from reservoirs near the Mendota site to extrapolate pressure and temperature gradients. Using a pressure gradient of 0.4339 psi/ft, CES estimates pore pressure to be 4,211 psi at the reference elevation. The initial temperature calculation uses two reference points (137.5°F at -6,350 ft and 249.7°F at -13,350 ft), above and below the target perforation zone, to define the initial temperature in between. Based on DOGGR/CalGEM data, the temperature gradient is 0.0146 °F/ft with the surface temperature set at 51.8 °F.

Initial formation salinity is set at 25,000 mg/L. DOGGR/CalGEM data show that in general, the salinity of Eocene and Cretaceous (Panoche formations are Cretaceous) range between 17,100 and 26,500 mg/L (narrative, page 59). Based on this information, 25,000 mg/L is an acceptable initial condition until more site-specific data are available.

The injection rate of 350,000 tons/year and the 20-year injection period are consistent with the narrative (page 71) and the operating details in Attachment A, which specify a proposed injection rate of 958.9 tons/day (349,998.5 tons/year).

Maximum injection pressure was calculated using the fracture gradient and reference depth, along with a safety margin. The fracture gradient is set at 0.65 psi/ft. Because there is currently no site-specific fracture pressure or fracture gradient in the injection and confining zones, CES used regional data from other sources. A study by Shryock (1968) cites a formation breakdown gradient in the San Joaquin Valley Basin range of 0.63-0.64 psi/ft at depths of 5,000 to 8,000 ft. It is noted that other sources based on studies within California have higher estimates for fracture gradient in the Coalinga district (0.7 and 0.96 psi/ft) (Attachment B pages 16-17). The 0.65 psi/ft. appears to be a reasonable initial estimate for this stage of the application process; the fracture pressure will be revised when a step-rate test has been conducted at this site.

Per the Class VI Rule, the maximum bottom-hole pressure may not exceed 90% of the fracture pressure; this equates to a maximum safe bottom-hole pressure gradient of 0.9×0.65 psi/ft = 0.585 psi/ft. Using the reference elevation of -9,505 ft, the fracture pressure is set at 5,677.4 psi.

2.4.6 Relative permeability and capillary pressure curves

In the absence of site-specific lab-based data (i.e., special core analysis or SCAL), the relative permeability/water saturation and capillary pressure/water saturation curves were developed using the Van Genuchten model (Attachment B, Table 2, Figure 7, page 13). Irreducible water saturation (Swir) was assumed to be 0.2 and 0.3 for sand and shale, respectively, and irreducible gas saturation was set at zero. Hysteresis was not considered for either relationship. This is acceptable as an initial step in developing a model.

CES notes that cores from the Mendota INJ_1 well will be subject to SCAL, which will allow the development of site-specific curves. This step will be important, as model predictions are

sensitive to the shape of the relative permeability-saturation functions used. Ideally, laboratory core-analysis techniques will be used for experimental measurement of the relative permeability-saturation and capillary pressure- saturation functions at site-specific reservoir conditions, with CO₂ and representative native fluids. If this is not feasible, relative permeability-saturation relationships may be estimated from core analysis using other immiscible fluids (e.g., Doughty et al., 2007). The inclusion or non-inclusion of hysteresis also affects the predicted migration of the CO₂ plume leading edge and predictions of residual trapping.

- Will experimental measurements be done at reservoir conditions, with CO₂ and native fluids?
 - *Yes, the laboratory measurement for the CO₂-brine relative permeability function will be performed at reservoir conditions. The salinity of the brine used in the experimental measurement will be prepared to represent the site-specific condition.*
- If it is not possible to obtain reliable laboratory-based data for the relative permeability and capillary pressure curves, will any changes be made to the estimation methods used in the current modeling effort?
 - *The sampling program will incorporate multiple redundant samples, including site-specific cores, to avoid failure in the laboratory testing. However, when the laboratory data are not available, other indirect site-specific information (e.g., irreducible water saturation derived from logs) can be used to update the parameters in the CO₂-brine relative permeability and capillary pressure function.*
- Will hysteresis be considered in model updates?
 - *Yes, the site-specific measurement from special core analysis (SCAL) will provide the information on the hysteresis and will be applied to the dynamic modeling.*
- The curves were developed for two rock types (sand and shale). Given the distribution of porosity/permeability clusters for the different formations (in Figure 30 of the narrative), is it possible a third set of curves will be needed (e.g., for the Fourth Panoche Sand if a backup injection zone is needed)? Will the same curves apply to both of the shale confining zones (First Panoche Shale and Moreno Shale)? (See also the question under “Porosity, permeability, and rock types” regarding the difference in porosity between the Second and Fourth Panoche and whether that might support a third rock type.)
 - *The rock types presented in Figure 30 of the narrative, which are updated in Figure 5, were used for fault seal analysis. The petrophysical property interpolations were completed on a zone-by-zone basis and did not use these facies types in the petrophysical modeling. For example, the unique petrophysical properties (Figure 3) for the Fourth Panoche Sand are accounted for in zone-specific petrophysical modeling. After well log data are acquired, the rock typing will be calculated using a more advanced methodology such as HRA. Likely, this analysis will focus on three to five different rock types, thus enabling characterization of the Second Panoche Sand and other potential injection sands. Different shale classes will be informed by core mineralogy and digital log responses for various shale seals such as the First Panoche Shale (primary) and Moreno Shale (secondary).*

2.4.7 Potential Pathways for Fluid Movement

2.4.7.1 Faults

The block diagram shown in the “Model Domain” file shows strata dipping to the SW, consistent with seismic images in the narrative that are based on 2D seismic data acquired by CES (Figures 16 through 19). Furthermore, the narrative, on page 15 states, “Near the proposed Mendota site, there are two known faults (USGS, 2019) located approximately 5 miles away.” See the site characterization evaluation included in EPA’s technical evaluation comments and information request dated August 19, 2020 for additional information.

All of these faults appear to be within the 19-mile grid of the model domain. However, the model as currently constructed does not include faults (“AoR Modeling” file), and their effects on fluid flow at the project site remain unexplored at this point due to a lack of data on fault stability and sealing properties. CES anticipates better fault assessment as new data are collected.

- Will any of the faults described in the narrative, especially Fault 13, be incorporated into the geomodel and the numerical model domain once they are better characterized (i.e., with respect to their depth, geometry, and sealing nature)?
 - *Yes, 3D seismic data will enable more accurate interpretation of faulting. The faulting picture is expected to change after interpretation of the more densely sampled 3D seismic data. Faults will be incorporated into a structural framework for dynamic simulation. Fault transmissibility will be calculated using the shale gouge ratio to predict fault permeability.*

2.4.7.2 Wells in the AoR

According to the Corrective Action plan (Attachment B, Section 5), there are 269 wells within a 2.5-mile radius of the Mendota INJ_1 well. This is based on information obtained from the California Natural Resources Agency well completion reports and the DOGGR/CalGEM Databases. Based on information about their depth or (where not available) their use, none are believed to penetrate the confining zone. Information based on the CalGEM online Well Finder database indicates that there are 5 oil and gas wells within 2.5 miles of the injection well; all were dry holes and were plugged. This information was independently verified for this review using searches of the online Well Finder database and well completion reports obtained from the California Natural Resources Agency.

Two wells, Amstar 1 and B.B. Co. 1 penetrate the Moreno Shale into the Panoche Sands. The Amstar 1 and B.B. Co. 1 wells are slated to be plugged, as described in the Corrective Action Plan.

2.4.8 Calculation of critical pressure

The PDF file submitted to the GSDT named “Critical-pressure-calc-01072020” contains the parameters, equation, and the resulting calculated critical pressure for the proposed injection well.

The calculation was done with Method 2 (Pressure front based on displacing fluid initially present in the borehole, which is applicable to hydrostatic case only) described in Section 3.4.1. (Determination of Threshold Pressure Front) of EPA’s Class VI Well Area of Review Evaluation and Corrective Action Guidance. The resulting delta P is 3.5 psi. An independent check on the calculations confirms the math is correct using the input values in the file (see the table below).

z_u	Garzas Reference Datum (ft)	-1415	Bottom of Garzas Formation
	Garzas Reference Datum (m)	-431	
z_i	Panoche Reference Datum (ft)	-9505	Top, Middle, & Bottom of Panoche Perforation Interval
	Panoche Reference Datum (m)	-2897	
P_u	Pressure in the USDW (Garzas, Psi)	701	
P_i	Pressure in the Panoche (Psi)	4,211	
$P_{u \text{ water}}$	Garzas fresh water density (kg/m3)	1000.0	
$P_{i \text{ brine}}$	Panoche brine density (kg/m3)	1002.0	
g	gravity (m/s2)	9.8066	
$\xi = \frac{\rho_i - \rho_u}{z_u - z_i}$	Density gradient	0.000811	

Without site-specific data, the inputs for the critical pressure calculation are from existing data from a nearby oil and gas field. The brine density of 1002.0 kg/m³ is consistent with an estimated salinity of 25,000 mg/L. The formation pressure of 4,211 psi at 9,505 ft is based on data from DOGGR/CalGEM.

It is understood that these data and the critical pressure calculation will be updated based on site-specific data collected during drilling of Mendota INJ_1 and OBS_1.

Calculation of the allowable threshold pressure increase using this method is applicable only for hydrostatic conditions. If site-specific fluid pressure and density measurements are not available, the *Area of Review Evaluation and Corrective Action Guidance* notes that it may be acceptable to calculate an initial critical pressure if available information suggests that the formation is likely hydrostatic.

CES has assumed a normal pressure gradient at this time based on initial reservoir pressure data from nearby oil and gas fields (as reported to DOGGR/CalGEM). These data suggest a pressure gradient of 0.4339 psi/ft. The normal pressure gradient will need to be confirmed based on the results of pre- operational testing. Should the results of this testing indicate that the formation is underpressurized, the allowable pressure increase may be greater than that calculated using the equation in the table. If it is overpressured, the allowable pressure increase would be smaller.

2.4.9 Representation of Fluid Properties

Relevant fluid properties for the numerical modeling include: viscosity, density, composition, and fluid compressibility. The table below presents the fluid properties as included in the permit application for the numerical modeling. These may be refined as site-specific data are collected (e.g., salinity and, therefore, density).

Parameter	Units	Evaluation Comments
Viscosity	M/LT	Calculated by modeling program. The CO ₂ gas viscosity is calculated per the methods described by Vesovic et al. (as cited in Fenghour, 1990) (Attachment B, page 6).
Density	M/L ³	Critical P calculations use 1,000 kg/m ³ for the USDW and 1,002 kg/m ³ for the Panoche. 1,002 kg/m ³ is consistent with the estimated/anticipated salinity of 25,000 mg/L (see narrative page 63 for estimated salinity). These agree with inputs in the AoR
Composition (salinity)	M/L ³	Narrative page 63 describes the basis for preliminary estimation of 25,000 mg/L salinity for the injection zone. More detailed chemistry was used for the geochemical modeling.
Fluid Compressibility	LT ² /M	Aqueous phase compressibility set to 0, and CO ₂ set as "compressible." (AoR modeling file).

- Why was the value for aqueous compressibility set to zero, and will this be changed in the next iteration of the model?
 - *The Aqueous Phase Compressibility Value field in the GSDT accepted only numeric values, not text. Therefore, in the Modeled Processes Comments field in the GSDT, CES included the following description of the compressibility of brine: "In Eclipse 300, the compressibility's of brine are based on Ezzokhis formula, which corrects the brine density for dissolved salt and CO₂." Therefore, "0" is used for aqueous phase compressibility value to indicate "Not Applicable."*

2.5 Model Calibration and Sensitivity Analyses

As the permit application narrative and Attachment B note, the preliminary model was developed based on limited site-specific data. There are currently no data available to use for model calibration or history matching. CES describes baseline data collection (e.g., via core sampling in INJ_1 and OBS_1) that will be used for model calibration. Attachment B (Section 3.2) states that the sensitivity analysis will be performed by varying one variable at a time.

A more complete review of this aspect of the modeling will be done once site-specific data are available from the testing program for calibration and sensitivity analyses.

- Please describe which variables will be manipulated in the sensitivity analysis and how the degree of variation for each variable will be determined.
 - *Uncertain parameters and their degree of uncertainty/variation for the sensitivity analysis will be evaluated and determined after site-specific data are collected. If a statistical variation from the samples cannot be determined, minimum and maximum values will be selected according to the possible ranges/uncertainties based on expert opinion.*
- How will model calibration be performed (e.g., manually or using a computer program)?
 - *Model calibration will be performed with the available testing program (e.g., step rate test and fall-off test) after the injection well is drilled. During the drilling operation, injection rates and corresponding downhole monitoring data (pressure, temperature, CO₂ saturation,*

and spinner survey) from injection and observation wells will be primarily used for model calibration. Because there is sufficient monitoring data available, a history matching workflow using the MEPO[®] multiple realization optimizer, or the Petrel Uncertainty & Optimization module can be applied.

2.6 Injection Zone Storage Capacity

CES used a simple volumetric approach to estimate storage capacity, using the number and sizes of cells in the geomodel along with the effective porosity assigned to each cell. Page 71 of the narrative states that, “Within a 2.5-mile radius of the Mendota_INJ_1, the total pore volume of the Second Panoche injection zone is calculated using the 3D geocellular model; for each model cell, the porosity was multiplied by the cell volume. The total pore volume was calculated to be 3.74x10⁶ ft³.” This is not an unreasonable approach for a general estimate of capacity given that site-specific data collection has not been done yet.

Some assumptions were not specified for this estimate.

- A density value for the CO₂ would have been needed to convert the desired number of tons to inject into volume to compare against the pore space. What value was used for the density of the supercritical CO₂, and how was it chosen?
 - *The initial storage capacity was reported incorrectly. CO₂ density was estimated from pressure and temperature gradients at the midpoints of both the First Panoche Sand and Second Panoche Sand zones. The pressure and geothermal gradients were obtained from nearby oilfield data (Schlumberger, Attachment B: Area of Review and Corrective Action Plan, 2020). Static storage capacity will be reassessed after formation-specific temperature and pressure are acquired. Updated storage capacity estimation results are shown in the table below.*

	<i>Temperature (°F)</i>	<i>Pressure (psi)</i>	<i>Density (kg/cm³)</i>	<i>Pore Volume (10⁶ m³)</i>	<i>P50 Millions Metric Tons</i>
<i>First Panoche Sand</i>	<i>177.2</i>	<i>3727</i>	<i>692.6</i>	<i>1466</i>	<i>20.3</i>
<i>Second Panoche Sand</i>	<i>187.6</i>	<i>4035</i>	<i>693</i>	<i>3000</i>	<i>41.58</i>

The CO₂ storage capacity depends on a combination of factors including multiphase flow processes, formation geometry and types of boundaries (e.g., open or closed boundaries, fault sealing), geologic parameters (e.g., porosity, permeability, compressibility) and their heterogeneity, and subsurface geochemistry. EPA’s *Class VI Geologic Site Characterization Guidance* also recommends considering trapping mechanisms. As additional data are collected, the simple volumetric approach can be updated and more refined estimates can be generated (e.g., through dynamic modeling).

- Does CES intend to incorporate additional considerations or use the dynamic modeling being conducted for AoR simulations to generate refined storage capacity estimates?
 - *Refinement of storage capacity estimates will be conducted after structure and petrophysical properties are updated with site-specific data. Storage capacity will be based on CO₂ density,*

pore volume, and AoR area.

- Please discuss the strengths and limitations of the approaches considered and clarify how storage estimates will be refined in the future as new data are available.
 - *The saline storage equation from the DOE considers 100% brine in the reservoir. It is possible that residual gas is present in the injection formation; however, this is not considered in the saline storage equation. Pressure and temperature data directly from the injection zone will provide a more accurate estimation of storage capacity. Storage estimates will be refined as new data are available from the drilling of a characterization well.*

2.7 Presentation of Model Results

Map and cross-sectional views of the simulated plume and pressure front were provided in the “AoRs” file submitted in the GSDT. The maps show the position of the plume and pressure front after 6 months, 5 years, and 20 years of injection, and 10 years, and 50 years post-injection. Figure 11 is CES’s proposed AoR as delineated by the simulation model.

The differences in the predicted position of the plume and pressure front between the cessation of injection, 10 years post-injection, and 50 years post-injection were fairly minor, suggesting that the plume movement may remain stable after injection ceases. Updated modeling when more data have been acquired will be needed to refine the modeled predictions.

2.8 AoR Reevaluation Schedule

CES described the procedures and timing for AoR reevaluations to be performed during the injection and post-injection phases. At this point in the permit application review, the five-year default reevaluation schedule appears to be appropriate. CES also identified events that would warrant an unscheduled AoR reevaluation, and EPA has the following questions and recommendations.

- Regarding reviewing available monitoring data for comparison to the model predictions, the specific types of data (e.g., the seismic methods to be used) will need to be refined as the injection and post-injection testing and monitoring strategies (in Attachments C and E) are finalized. EPA also recommends the following revisions to these planned reviews:
 - Reviews of available data on the position of the CO₂ plume and pressure front should reference analysis of fluids sampled in OBS1.
 - Reviews of ground water chemistry monitoring data should reference data from ACZ1 in addition to the shallow monitoring wells and USDW1.
- *In the updated version of Attachment B (Schlumberger, Attachment B: Area of Review and Corrective Action Plan, 2020), the above data reviews will be added.*
- EPA recommends including additional triggers for unscheduled AoR reevaluations:
 - If the arrival time of the plume and/or pressure front at OBS_1 and/or when pressure and plume data recorded at OBS1 differs significantly from modeled projections.
 - Initiation of competing Panoche Formation injection projects within the same

injection formation within a 1-mile radius of the injection well.

- Significant land use changes that would affect site access.
- *The above EPA recommended triggers will be added to the updated version Attachment B (Schlumberger, Attachment B: Area of Review and Corrective Action Plan, 2020).*
- What is the timing for initiating an AoR reevaluation that is triggered based on the events described (e.g., within one month of identifying the existence of the event)?
 - *After a triggering event is identified, investigated, and confirmed, an AoR reevaluation will be completed. The exact timing of an AoR reevaluation will vary depending on the triggering events in section 6.2 of Attachment B (Schlumberger, Attachment B: Area of Review and Corrective Action Plan, 2020); however, a 1-month timeframe is likely. CES will discuss any such events with the UIC Program Director to determine if an AoR reevaluation is required.*
- Please remove pressure from the list of hydrochemical/physical parameters identified immediately above the confining zone, as pressure will not be monitored in ACZ1.
 - *Pressure monitoring with other tools above the confining zone is designed to monitor leakage of brine and/or CO₂ past the Moreno seal. It was described in the page 7 in Attachment C.*

2.9 Post-Injection Site Care Plan

Certain elements of CES's Post-Injection Site Care and Site Closure Plan (Attachment E) are based on the modeling effort and results and are evaluated below.

As required at 40 CFR 146.93(a)(2)(i) and (ii), CES presented the pre- and post-injection pressure differential and provided a map that illustrates the predicted positions of the CO₂ plume and associated pressure front at site closure.

Figure 1 of Attachment E shows the predicted extent of the CO₂ plume and pressure front (1Pc=3.5psi) at site closure. This map and cross-sectional view match the "After 10-year Post-Injection" figure in the "AoRs" file submitted in the GSDT. (See the section on Presentation of Model Results above.) This figure will need to be updated as needed based on the results of the updated modeling that will be performed as additional site data are collected.

2.9.1 Post-Injection Site Care Time Frame

CES proposed a 10-year alternative post injection site care time frame but did not provide a justification for the appropriateness of the 10-year time frame that addresses the criteria at 40 CFR 146.93(c). CES notes that the Post Injection Site Care Plan will be finalized based on the results of updated modeling performed after pre-operational testing is complete.

As discussed under "Presentation of Model Results," the differences in the predicted position of the plume and pressure front between the cessation of injection, 10 years post-injection, and 50 years postinjection were fairly minor, suggesting that the plume movement may remain stable after injection ceases, which may justify a 10-year post-injection site care timeframe. Future versions of Attachment E will need to address each of the criteria at 40 CFR 146.93(c) based on the site-specific data collected.

This discussion will be revised as necessary during the review of the pre-operational phase AoR modeling.

2.9.2 Non-Endangerment Demonstration Criteria

In Section 6 of the Post-Injection Site Care and Site Closure Plan, CES described the contents of a non-endangerment demonstration report that would contain: a summary of existing monitoring data; computational modeling history; and evaluations of reservoir pressure, the CO₂ plume, and emergencies or other events. The following recommendations are offered to provide for a set of criteria that are as specific as possible and can be supported by the data CES will collect during injection and post-injection testing and monitoring. It is recognized that several related parts of the project are under development (e.g., testing and monitoring activities, AoR modeling); however, these recommendations are offered to reduce future uncertainty.

- The criteria should specify that the same delineation model that supported the initial AoR delineation will be used in future reevaluations and to make the non-endangerment demonstration to facilitate verification and/or model calibration using actual monitoring and operational data.
 - *The methods used for delineating AoR will be consistent throughout the life of the project including the non-endangerment demonstration and will be specified in the updated version of Attachment B (Schlumberger, Attachment B: Area of Review and Corrective Action Plan, 2020).*
- The criteria should discuss the predicted behavior of the CO₂ plume and pressure front, supported by maps and graphs (e.g., of pressure profiles or extent of the plume and pressure front) in the context of the data that will be collected to demonstrate that the plume and pressure front are behaving as predicted at various points in time.
 - *This will be added to the updated version of non-endangerment demonstration criteria in Attachment B (Schlumberger, Attachment B: Area of Review and Corrective Action Plan, 2020).*
- The data that will support the non-endangerment demonstration should be consistent with the final injection and post-injection phase testing and monitoring strategies in Attachments C and E. For example, the geophysical methods selected (i.e., 2D vs. 3D seismic surveys) should be consistent. They should also be specific as to the types/locations of data that will be gathered and compared against the model prediction to facilitate model validation (e.g., the formations for which groundwater quality data will be collected and pressure monitoring locations).
 - *The 2D seismic data mentioned in Attachment C was purchased in 2019 and used for the initial structure mapping. All subsequent seismic acquisition will be 3D. An initial 3D surface seismic survey will be conducted to more accurately characterize the subsurface structure. For subsequent monitoring, a 3D vertical seismic profile (VSP) may be substituted for a 3D surface seismic survey if this is acceptable to the EPA. If this was to be proposed, it would be discussed with the EPA first.*
- The criteria should include an evaluation of natural and artificial potential conduits for fluid movement, including the faults described in the geologic narrative.
 - *A clearer picture of the faulting at the site will be established after the 3D seismic data are acquired and interpreted, and the positions of the faults will be registered with the microseismic monitoring program. The location of microseismic events will be compared to*

the locations of the interpreted faulting from the 3D seismic data. This information will be included in Section 6.6 in Attachment E (Schlumberger, Attachment E: Post-Injection Site Care and Site Closure Plan, 2020).

- The non-endangerment criteria should include evaluations of mobilized fluids and passive seismic data. It appears that the discussion in Section 6.6 addresses these evaluation areas.
- The non-endangerment criteria should include a summary of any emergencies or other unanticipated events that may occur during the injection and post-injection phases. This may be presented in a table that shows (1) examples of unanticipated events that might occur, and (2) the types of data that might be used to demonstrate that any associated issues have been resolved such that there is no endangerment to USDWs.
 - *CES will incorporate the recommendations into future versions of Attachment E (Schlumberger, Attachment E: Post-Injection Site Care and Site Closure Plan, 2020).*

3 Appendix A: Updated Tables and Figures

Table 2: Proposed operational procedures.

Parameters/Conditions	Limit or Permitted Value	Unit
Maximum Injection Pressure		
Surface	2026	psi
Downhole	5677	psi
Average Injection Pressure		
Surface	1042	psi
Downhole	4212	psi
Maximum Injection Rate	958.9	tons/day
Average Injection Rate	958.9	tons/day
Maximum Injection Volume and/or Mass	350000	tons/year
Average Injection Volume and/or Mass	350000	tons/year
Annulus Pressure	5777	psi
Annulus Pressure/Tubing Differential	100	psi

2. Injection Well Operating Conditions

PARAMETER/CONDITION	LIMITATION or PERMITTED VALUE
Maximum Injection Pressure - Surface	2026 psig
Maximum Injection Pressure - Bottomhole	5677 psig
Annulus Pressure	5777 psig
Annulus Pressure/Tubing Differential	100 psig
Maximum CO ₂ Injection Rate	958.9 tons/day

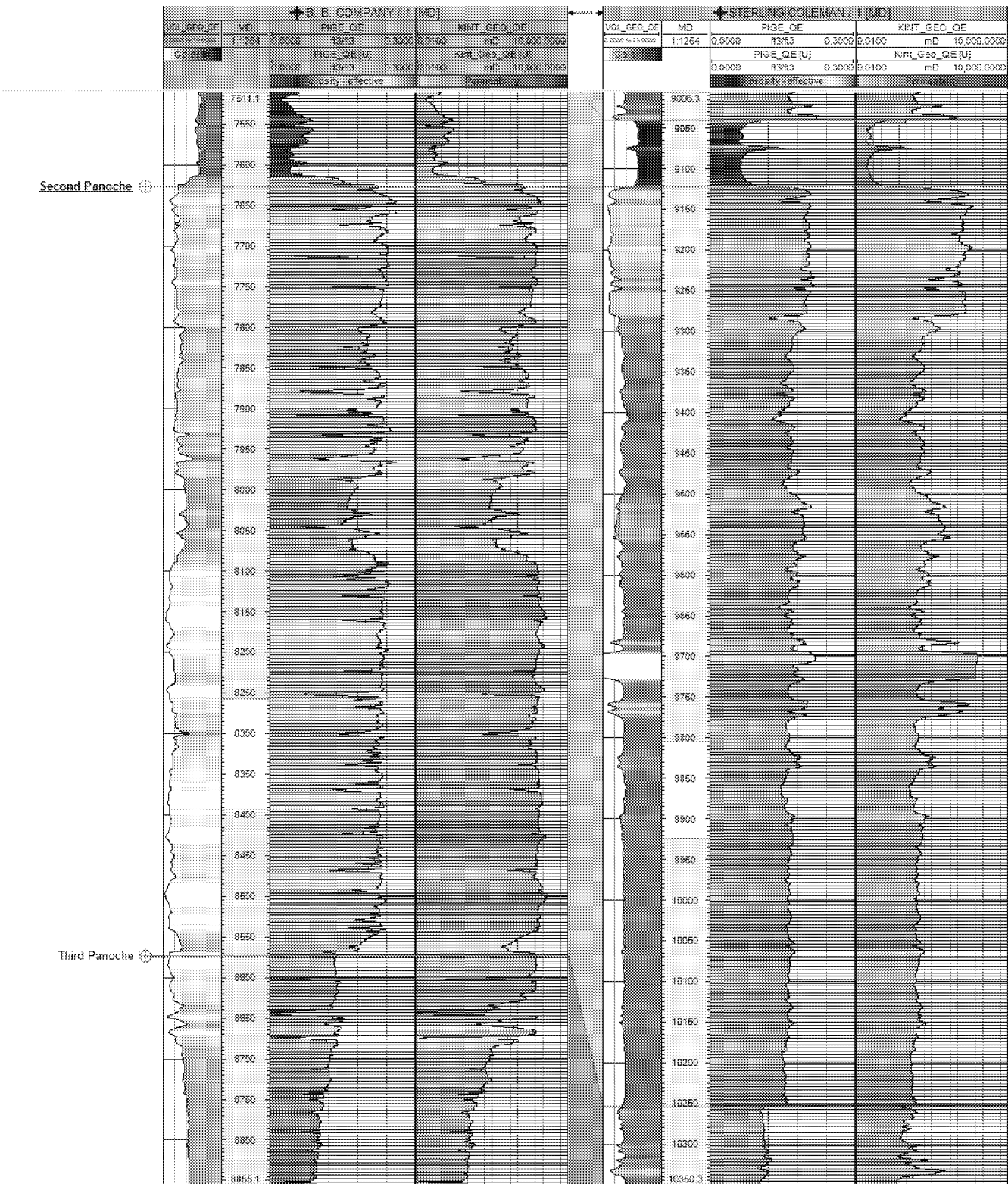


Figure 1: Well log upscaling of the two nearest wells over the Second Panoche Sand (from Petrel 2019).

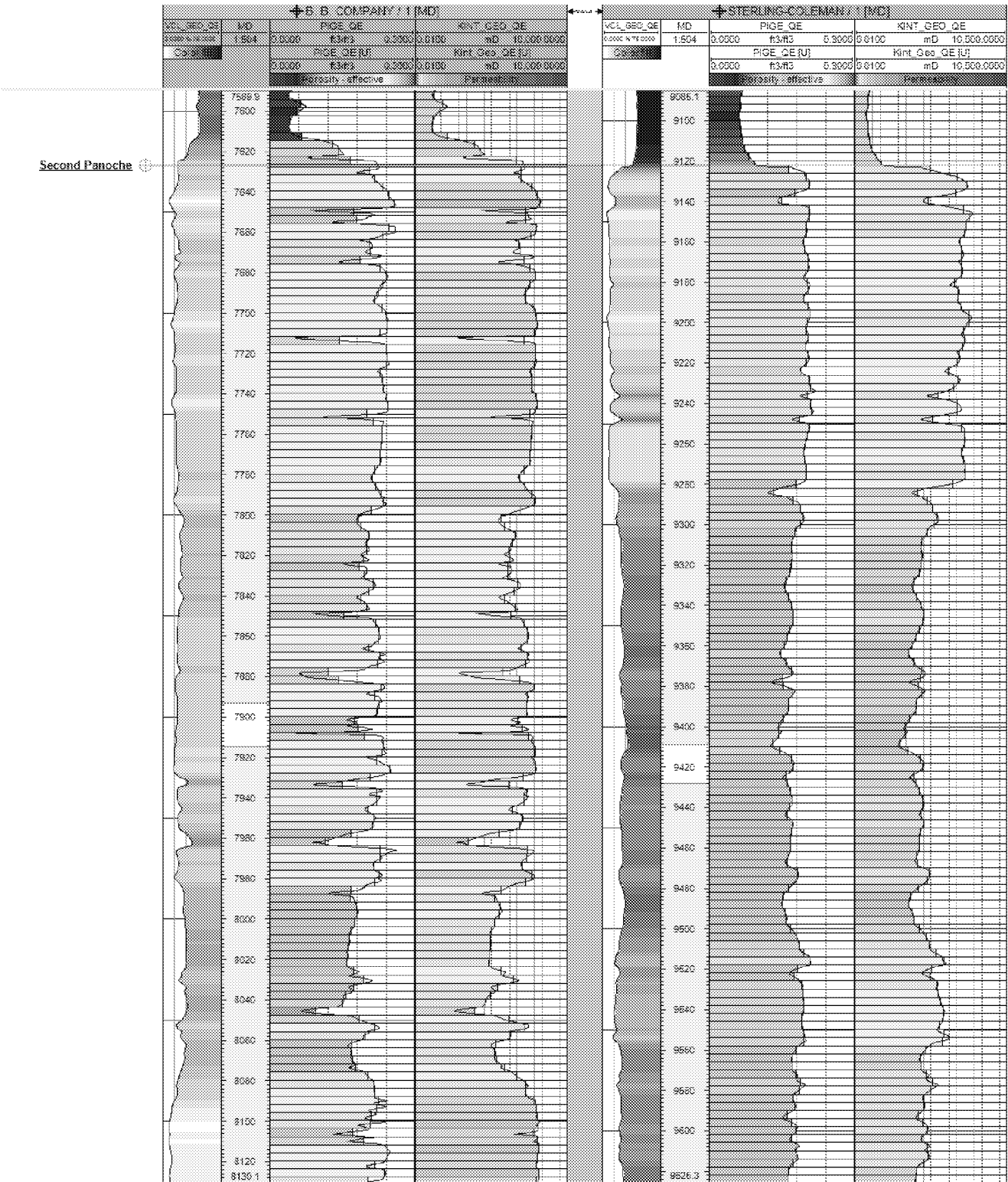


Figure 2: Well log upscaling of the two nearest wells over the upper section of the Second Panoche Sand (from Petrel 2019).

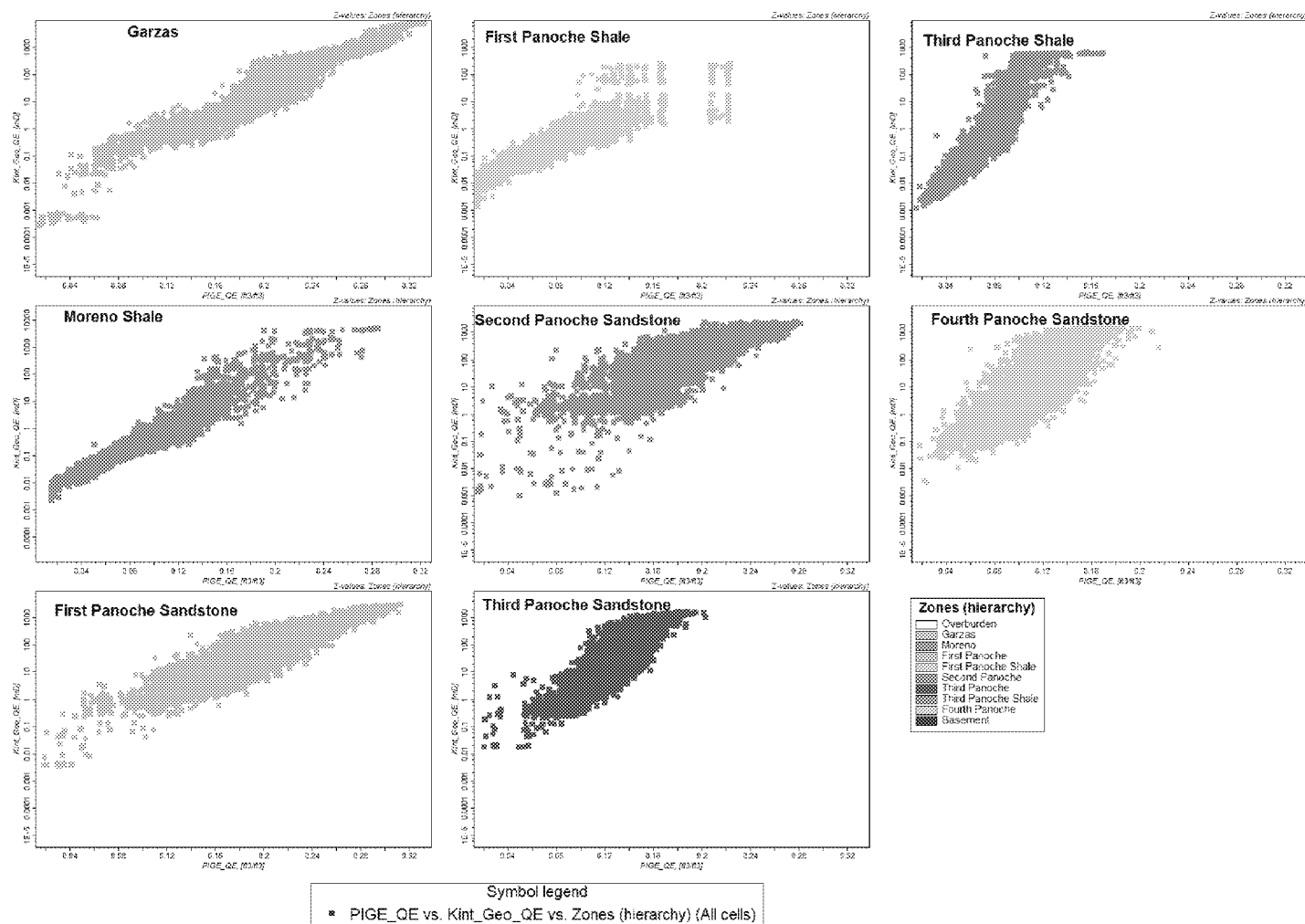


Figure 3: Porosity-permeability crossplot model cells colored by formation (from Petrel 2019).

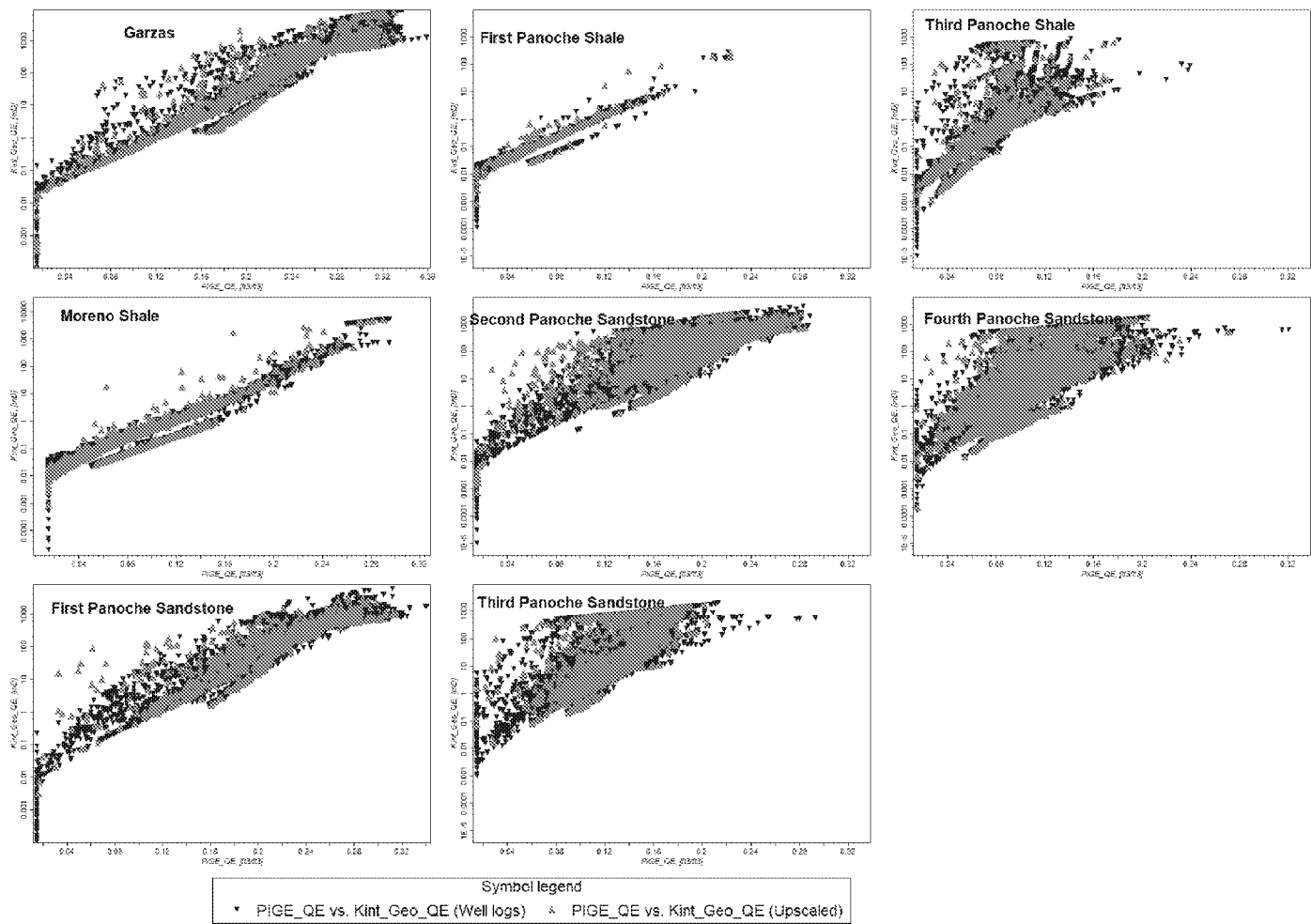


Figure 4: Porosity-permeability crossplots of well logs and upscaled cells (from Petrel 2019).

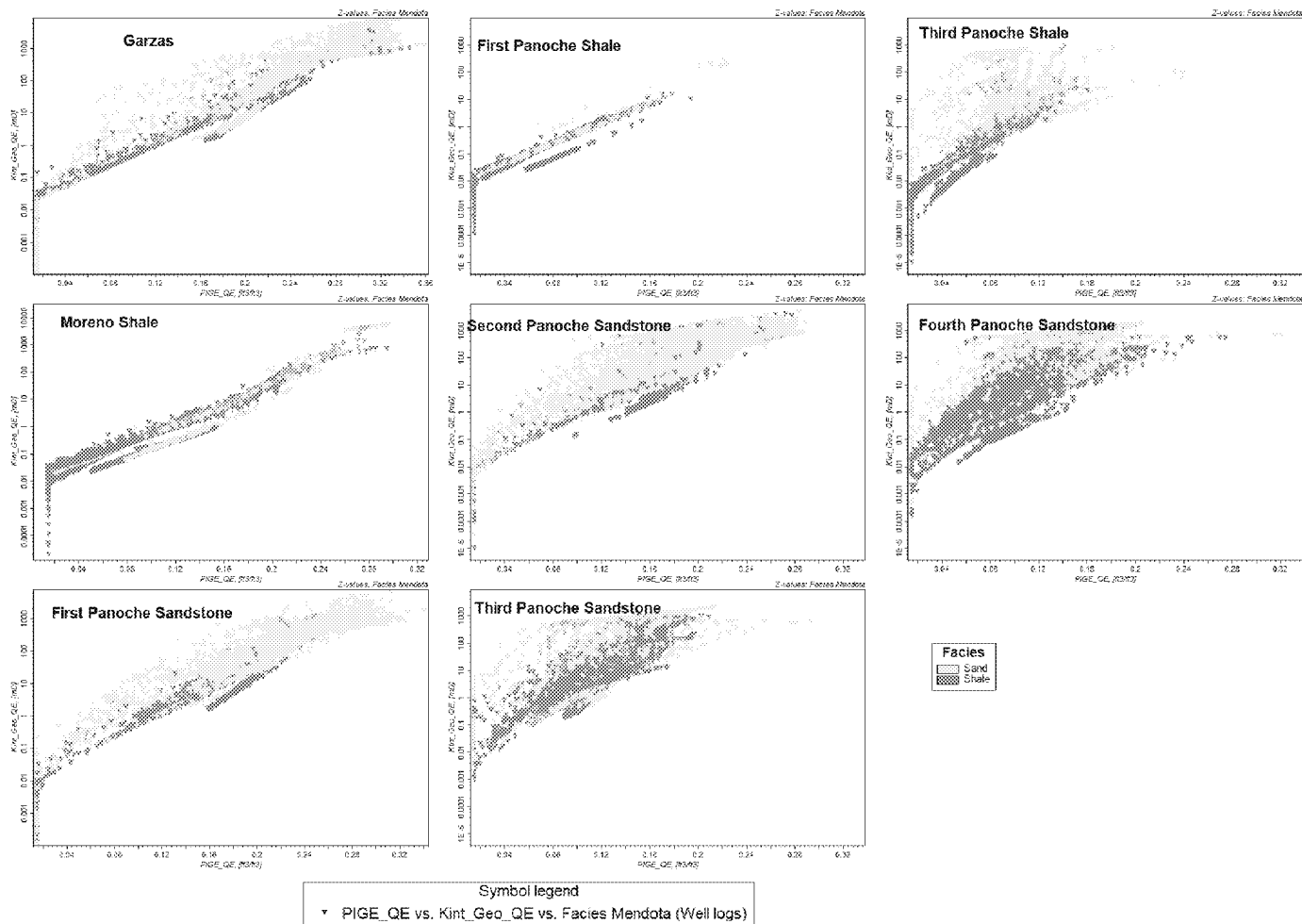


Figure 5: Porosity-permeability crossplots of well logs vs. facies type (sand and shale) (from Petrel 2019).

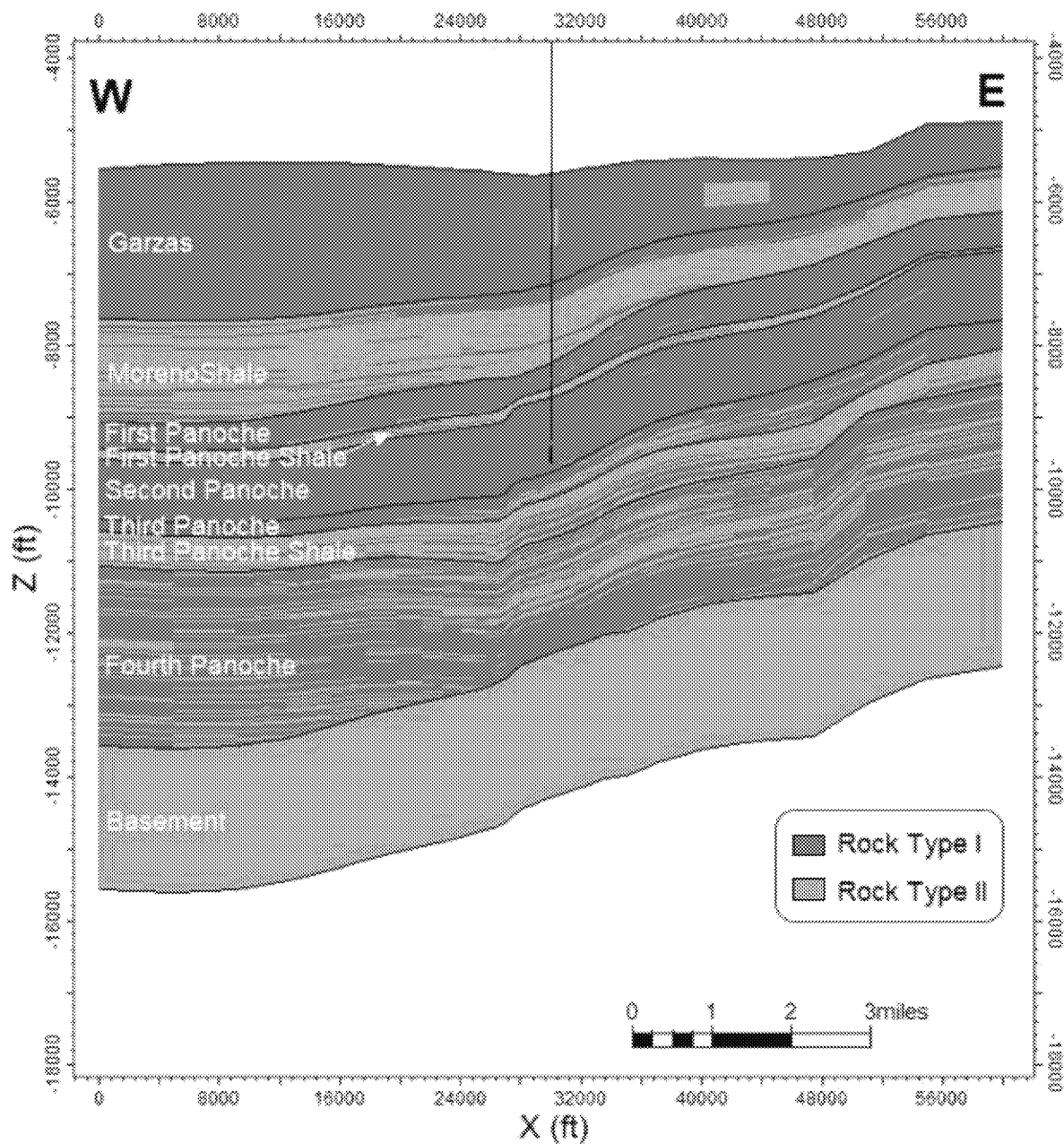


Figure 6. Rock types along the E-W cross section (from Petrel 2019).

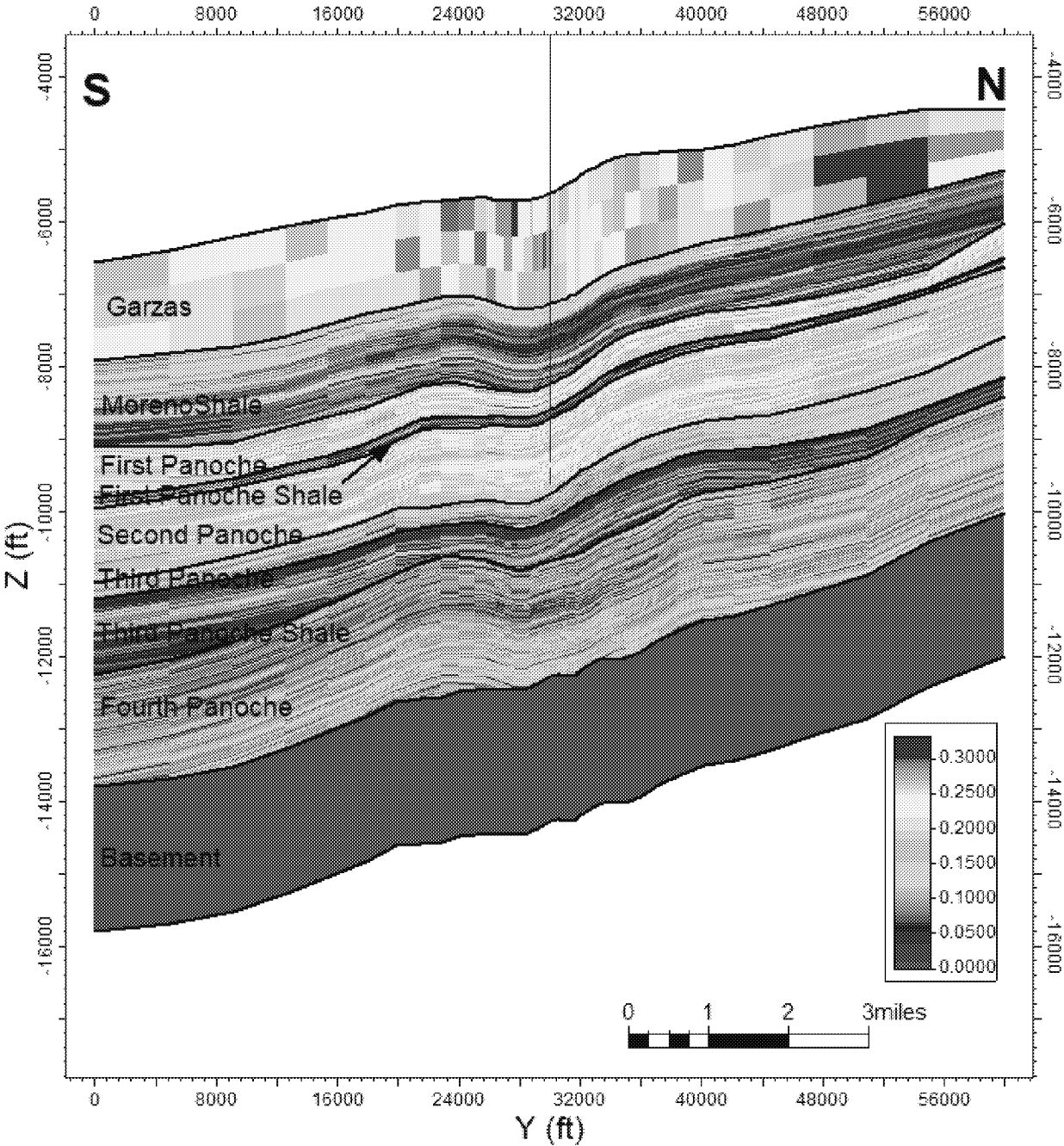


Figure 7. Upscaled porosity profile along the N-S cross-section.

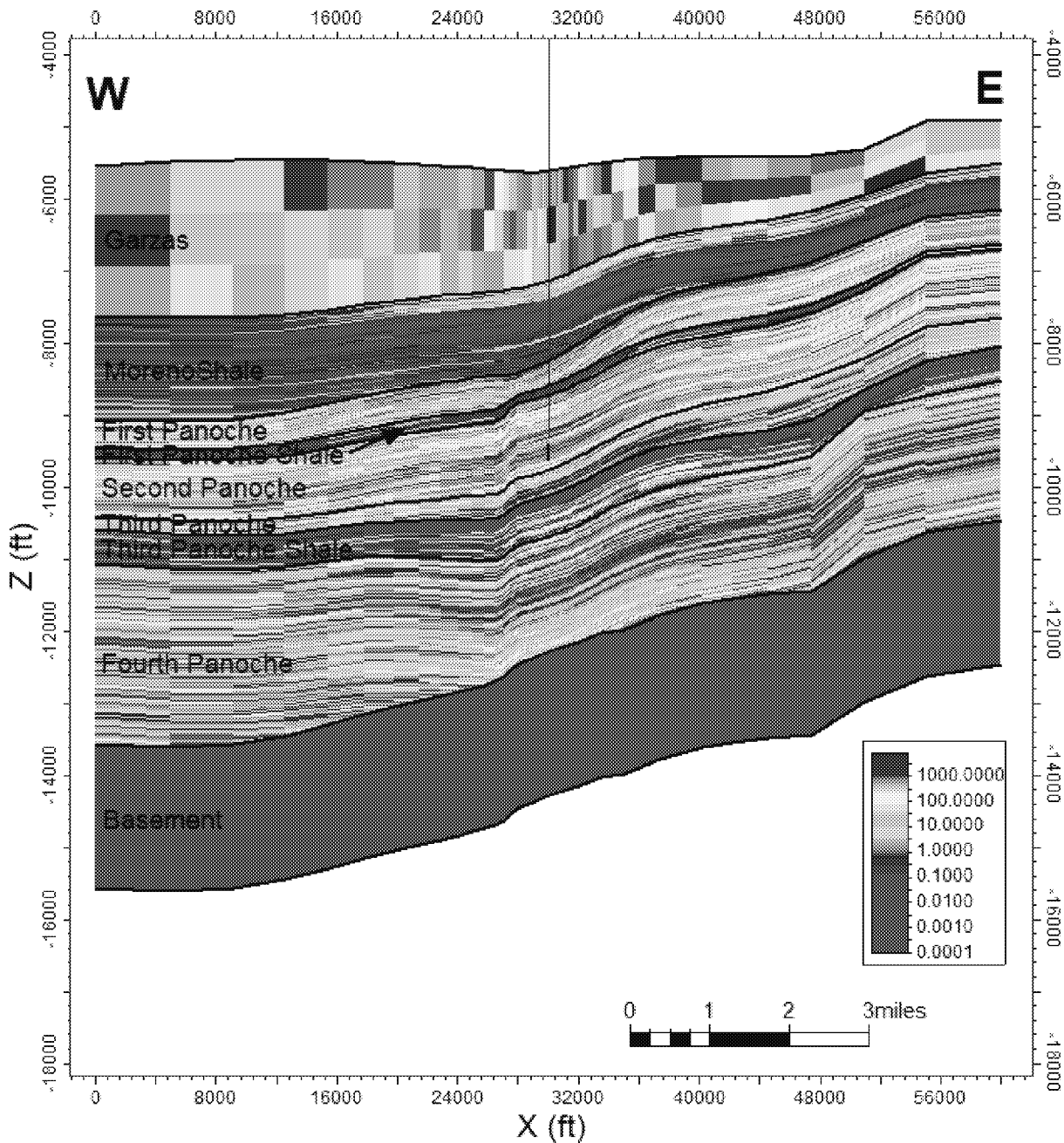


Figure 8. Upscaled permeability profile along the E-W cross-section.